Chinese Chemical Letters 35 (2024) 109058

Contents lists available at ScienceDirect

Chinese Chemical Letters

journal homepage: www.elsevier.com/locate/cclet

Chemoselective electrochemical seleno-cyclization of dienes to medium-sized benzo[*b*]azocines

Zhichuan Wang[a], Xin Wang[a], Quanxin Li[b], Shaofei Ni[b,*], Dongyang Zhao[a], Shubin Yang[a], Ge Qiu[a,c,*], Kai Sun[a,*]

[a] *College of Chemistry and Chemical Engineering, Yantai University, Yantai 264005, China*
[b] *Department of Chemistry and Key Laboratory for Preparation and Application of Ordered Structural Materials of Guangdong Province, Shantou University, Shantou 515063, China*
[c] *Aix Marseille Univ., CNRS, Centrale Marseille, iSm2, Marseille, France*

ARTICLE INFO

Article history:
Received 23 April 2023
Revised 29 August 2023
Accepted 5 September 2023
Available online 10 September 2023

Keywords:
Medium-sized *N*-heterocycles
Electrocatalysis
Radical
Mechanistic insights
Selenylation

ABSTRACT

The preparation of medium-sized benzo[*b*]azocines has always been challenging because of inherently unfavorable enthalpy and entropy factors. This report presents a novel approach for accessing 8-membered seleno-benzo[*b*]azocines *via* electrochemically-driven seleno-cyclization. This method enables room-temperature preparation of various structurally diverse medium-sized seleno-benzo[*b*]azocines. The facile deselenation of the seleno-cyclization products to generate functionalized dienes is an additional benefit of this indispensable reaction. Mechanistic insights are presented based on radical inhibition experiments and cyclic voltammetry measurements, which elucidate the radical pathway. Finally, density functional theory calculations further rationalize the rate-determining step and the unique chemoselectivity observed in this transformation.

Medium-sized molecular ring structures, particularly 8-membered benzo[*b*]azocines, are prominent structural motifs that are found in many natural products and bioactive molecules (Fig. 1) [1–8]. These ring structures tend to exhibit unique biological activities as analgesic or sedative agents that affect the central nervous system. However, synthesizing 8-membered benzo[*b*]azocines is difficult, owing to several inherently unfavorable enthalpic and entropic barriers associated with the transition states leading to medium-sized rings [9–14]. In recent decades, steady progress has been made in the preparation of medium-sized benzo[*b*]azocine frameworks, with cycloaddition [15–25] and ring closing metathesis [26–28], representing the most straightforward routes to these 8-membered *N*-heterocycles. Nevertheless, most available synthetic procedures require noble transition metal catalysts or unstable starting materials. Therefore, novel strategies should be developed for the facile preparation of medium-sized benzo[*b*]azocines.

Organoselenium compounds, especially selenium-containing *N*-heterocycles, are important molecules owing to their roles in medicine and materials science [29–36]. Therefore, significant research efforts have been devoted to exploring practical methods for synthesizing selenium-functionalized heterocycles [37]. In particular, selenium-centered radical-initiated tandem cyclization at unsaturated bonds represents a valuable strategy for preparing selenium-containing *N*-heterocycles [38–45]. Recently, electrochemical seleno-cyclization across unsaturated bonds [46–50] has demonstrated utility as an environmental-friendly strategy [51,52] for constructing such heterocycles using only electrons to provide the reaction driving force. Moreover, the electrical potential can be precisely controlled during the required electrochemical process, which enables acute manipulation of the chemoselectivity and reactivity [53–56]. Building upon our group's work related to nitrogen heterocyclic chemistry [57–61], herein we designed a diene system comprising *N*-(but–3-en-1-yl)–2-vinylanilines and explored electrochemical selenium-centered radical-initiated tandem cyclization. This approach involved unique chemo- and regioselective addition with 8-endo cyclization to obtain a series of 8-membered benzo[*b*]azocine derivatives. Previous reports have described energetically favorable seleno-radical-based addition cyclizations to selenium-containing 5- or 6-membered *N*-heterocycles (Scheme 1a) or ionic cycloaddition and ring closing metathesis strategies. However, to our knowledge, this article presents the first successful example of radical-triggered ordered addition involving an 8-*endo* cyclization reaction to prepare medium-sized seleno-benzo[*b*]azepines (Scheme 1b).

* Corresponding authors at: College of Chemistry and Chemical Engineering, Yantai University, Yantai 264005, China.
E-mail addresses: sfni@stu.edu.cn (S. Ni), gegeqiu@sina.com (G. Qiu), sunk468@nenu.edu.cn (K. Sun).

https://doi.org/10.1016/j.cclet.2023.109058
1001-8417/

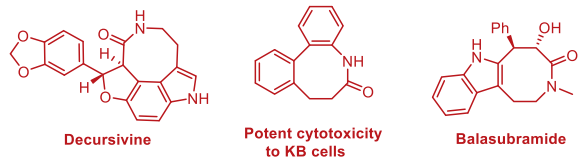

Fig. 1. Selected azocinone moieties found in bioactive molecules and natural products.

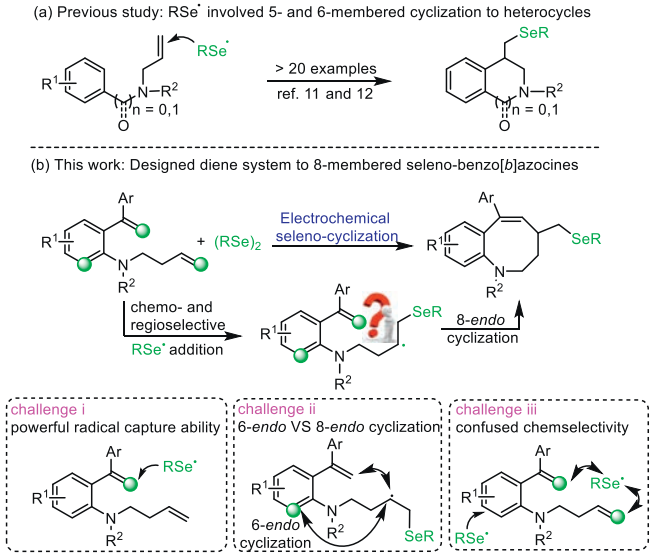

Scheme 1. RSe˙-triggered addition cyclization to obtain seleno-heterocycles.

To achieve this goal, critical challenges that originate from the multiple substrate reactive sites and the energetics of cyclization need to be overcome. For example, the diphenylethylene fragment in diene molecules is a powerful radical inhibitor with strong radical trapping capabilities. Therefore, the seleno-radicals generated *in situ* are likely to be trapped, thereby terminating the reaction (challenge i). Additionally, in terms of thermodynamics, the secondary carbon radical intermediate might be inclined toward 6-*endo* cyclization to afford an undesirable quinoline scaffold (challenge ii). Finally, considering the two alkenyl groups (activated and unactivated) in the diene system, directing the chemoselective addition of seleno-groups to both double bonds is difficult (challenge iii).

To determine the optimal reaction conditions for the proposed chemo- and regioselective seleno-cyclization, we first carried out the reaction using *N*-(but-3-en-1-yl)−4-methyl-*N*-(2-(1-phenylvinyl)phenyl)benzenesulfonamide **1a** and diphenyl diselenide **2a** as model substrates. As shown in Table 1, Pt(+)/Pt(−) were selected as the anode and cathode, respectively, with $^{n}Bu_4NBF_4$ as the supporting electrolyte. The test reaction was performed in 1,2-dichloroethane (DCE) at room temperature under a constant current of 2 mA in an undivided three-necked flask for 3 h, and under these conditions, the target **3a** could be isolated in 33% yield (entry 1). We then tested other common electrolytes, including $^{n}Bu_4NI$, $^{n}Bu_4NPF_6$, and $^{n}Bu_4NClO_4$. The results indicated that $^{n}Bu_4NPF_6$ exhibited the most positive effect, leading to an isolated yield of **3a** of 47% (entry 3), whereas reactions with $^{n}Bu_4NI$ and $^{n}Bu_4NClO_4$ did not proceed efficiently (entries 2 and 4, respectively). Solvent screening revealed that *N*,*N*-dimethylformamide (DMF), tetrahydrofuran (THF), and methanol (MeOH) were not ideal for this transformation (entries 5–7), while dichloromethane (DCM) gave a satisfactory yield of **3a** up to 60% (entry 8). The impacts of the electrode materials were also explored; however, lower reaction yields were obtained when the Pt(+)/Pt(−) electrodes were replaced with C(+)/C(−) or C(+)/Pt(−) (entries 9 and 10).

Table 1
Optimization of reaction conditions.[a]

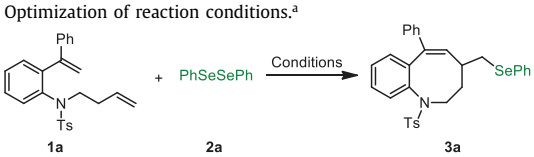

Entry	Electrolyte	Solvent	Electrodes	Isolated yield (%)
1	$^{n}Bu_4NBF_4$	DCE	Pt(+)/Pt(−)	33
2	$^{n}Bu_4NI$	DCE	Pt(+)/Pt(−)	0
3	$^{n}Bu_4NPF_6$	DCE	Pt(+)/Pt(−)	47
4	$^{n}Bu_4NClO_4$	DCE	Pt(+)/Pt(−)	17
5	$^{n}Bu_4NPF_6$	DMF	Pt(+)/Pt(−)	0
6	$^{n}Bu_4NPF_6$	THF	Pt(+)/Pt(−)	0
7	$^{n}Bu_4NPF_6$	MeOH	Pt(+)/Pt(−)	0
8	$^{n}Bu_4NPF_6$	DCM	Pt(+)/Pt(−)	60
9	$^{n}Bu_4NPF_6$	DCM	C(+)/C(−)	0
10	$^{n}Bu_4NPF_6$	DCM	C(+)/Pt(−)	27
11[b]	$^{n}Bu_4NPF_6$	DCM	Pt(+)/Pt(−)	57
12[c]	$^{n}Bu_4NPF_6$	DCM	Pt(+)/Pt(−)	53
13[d]	$^{n}Bu_4NPF_6$	DCM	Pt(+)/Pt(−)	58
14[e]	$^{n}Bu_4NPF_6$	DCM	Pt(+)/Pt(-)	0

[a] Reaction conditions unless otherwise noted: **1a** (0.2 mmol), **2a** (0.2 mmol), supporting electrolyte (0.4 mmol), solvent (6 mL), 2 mA constant current, room temperature, 12 h.
[b] Reaction performed at 4 mA.
[c] $^{n}Bu_4NPF_6$ (1.0 equiv.).
[d] $^{n}Bu_4NPF_6$ (3.0 equiv.).
[e] Without electricity.

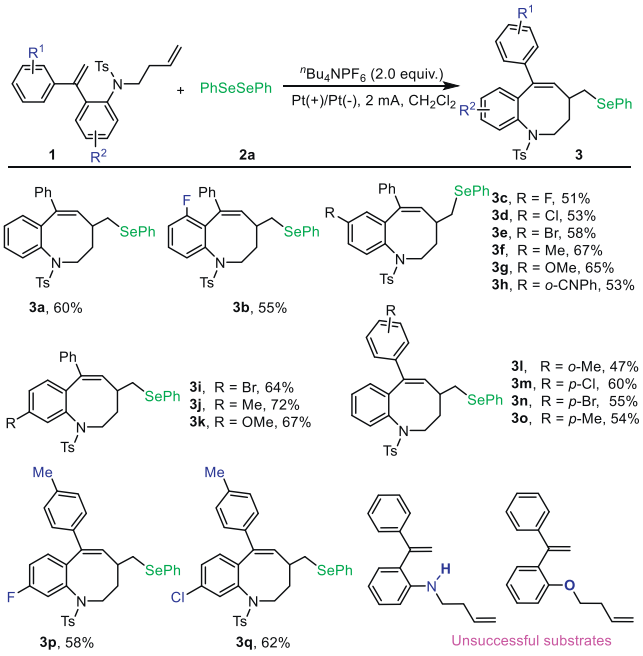

Scheme 2. Diene substrate scope. Reaction conditions: **1** (0.2 mmol), **2a** (0.2 mmol), supporting electrolyte $^{n}Bu_4NPF_6$ (0.4 mmol), 2 mA constant current, DCM solvent (6 mL), room temperature, 12 h, isolated yields are reported.

Moreover, the yield was not improved appreciably when changing the constant current to 4 mA or appropriately modifying the amount of electrolyte (entries 11−13). A control experiment also confirmed that the desired product **3a** was not generated without electricity (entry 14).

Next, we used the optimized reaction conditions to examine the substrate scope for the seleno-cyclization of 8-membered seleno-benzo[*b*]azocines (Scheme 2). Substrates with electron-withdrawing (3-F, 4-F, 4-Cl, 4-Br, 5-Br) or electron-donating groups

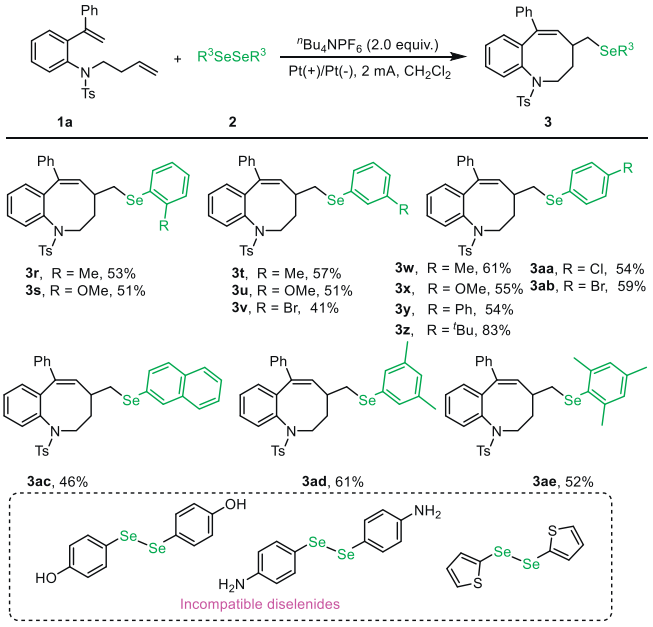

Scheme 3. Diselenide substrate scope. Reaction conditions: **1a** (0.2 mmol), **2** (0.2 mmol), supporting electrolyte $^{n}Bu_4NPF_6$ (0.4 mmol), 2 mA constant current, DCM solvent (6 mL), room temperature, 12 h, isolated yields are reported.

(4-Me, 4-OMe, 4-*p*-CNPh, 5-Me, 5-OMe) on the phenyl ring of the aniline moiety were compatible with this reaction; the transformation proceeded smoothly to afford the corresponding 8-membered seleno-benzo[*b*]azocines **3b**–**3k** in 51%–72% yields. Next, we investigated how substituents on the alkene-tethered phenyl ring influenced the reaction. Substrates bearing *o*-Me, *p*-Cl, *p*-Br, and *p*-Me groups on the phenyl were all compatible with this conversion, giving the corresponding products **3l**–**3q** in 47%–62% yields. When the *N*-Ts moiety was replaced with *N*–H, the seleno-cyclization did not occur.

We further explored the diselenide substrate scope of the seleno-cyclization reaction. As shown in Scheme 3, diselenides bearing electron-donating (–Me, –OMe, –Ph, –^{t}Bu) and electron-withdrawing substituents (–Cl, –Br) at various positions on the phenyl ring were all compatible with the reaction, and the corresponding seleno-cyclization products **3r**–**3ab** were isolated in moderate to high yields (41%–83%). Steric effects did not appear to impact the seleno-cyclization process because diselenides with *o*-, *m*-, and *p*-Me groups on the phenyl ring proceeded smoothly, and no appreciable yield disparity was observed (**3r**, **3t**, and **3w**). Furthermore, 1,2-di(naphthalen-2-yl)diselane and multi-substituted 1,2-bis(3,5-dimethylphenyl)diselane and 1,2-dimesityldiselane were also suitable substrates for this transformation; the corresponding products **3ac**, **3ad**, and **3ae** were obtained in 46%, 61%, and 52% yields, respectively. Diselenides with –OH, –NH_2, and thiophene substituents were incompatible with this electrochemically-driven transformation.

Importantly, the facile conversion of seleno-groups to other functional groups renders selenation reactions indispensable. Treating seleno-benzo[*b*]azepine **3a** with *m*-chloroperbenzoic acid (*m*-CPBA) or H_2O_2 generated the desired deselenation product **4** *via* oxidation-elimination under mild conditions. This result indicated the potential for further synthetic transformations, such as hydroxylation, oxidation, difunctionalization, and epoxidation (Scheme 4) [62–65].

Control experiments were performed to gain mechanistic insights regarding this seleno-cyclization reaction (details in Supporting information). First, when a stoichiometric amount of a radical scavenger, *e.g.*, 2,2,6,6-tetramethyl-1-piperidinyloxy (TEMPO,

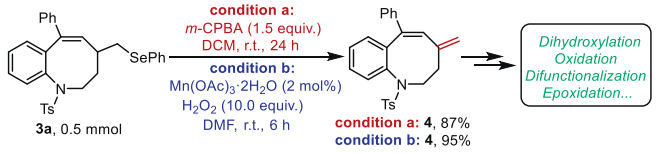

Scheme 4. Deselenation investigations.

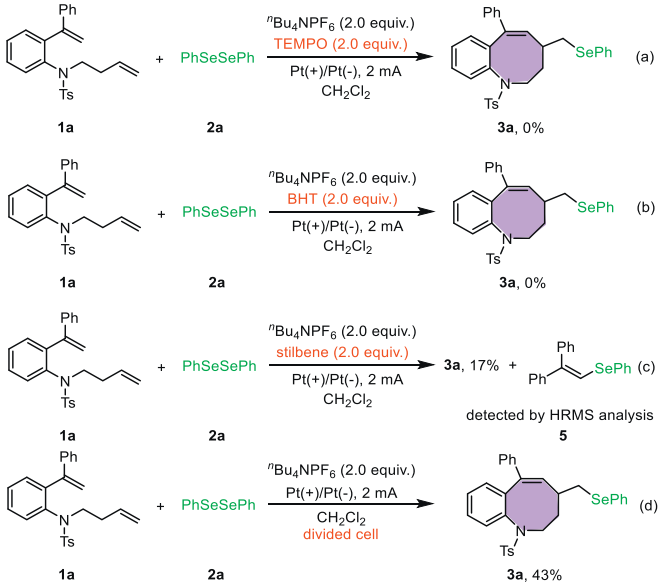

Scheme 5. Control experiments.

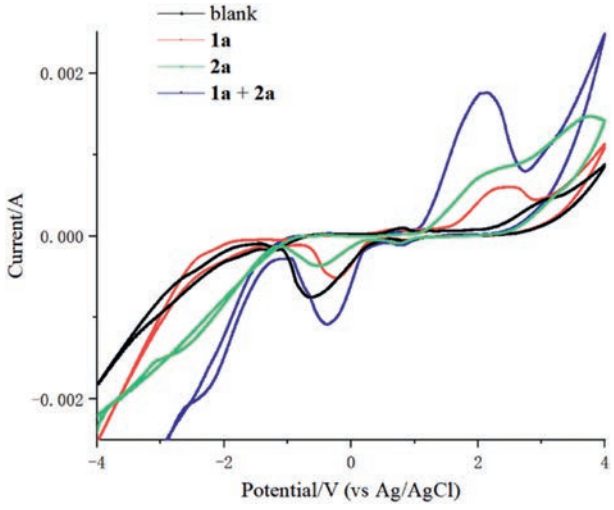

Fig. 2. Cyclic voltammetry results.

2.0 equiv.) or 2,6-di–*tert*–butyl–4-methylphenol (BHT, 2.0 equiv.) was added into the standard reaction system, the seleno-cyclization was remarkably inhibited, such that substrate **1a** was recovered (Schemes 5a and b). When stilbene (2.0 equiv.) was added, only 17% of **3a** could be isolated, and the radical-trapping product **5** was detected *via* high resolution mass spectrometry (HRMS) analysis (Scheme 5c). These results suggest that the transformation may proceed through a radical-type mechanism involving a seleno-centered radical. We also conducted a control experiment in a divided cell, and product **3a** was detected following anodic oxidation (isolated yield = 43%; Scheme 5d), indicating that the reaction could be completed directly at the anode.

Cyclic voltammetry (CV) experiments were also performed using **1a** and **2a** (Fig. 2). The oxidation peak of **1a** appeared at 2.00 V,

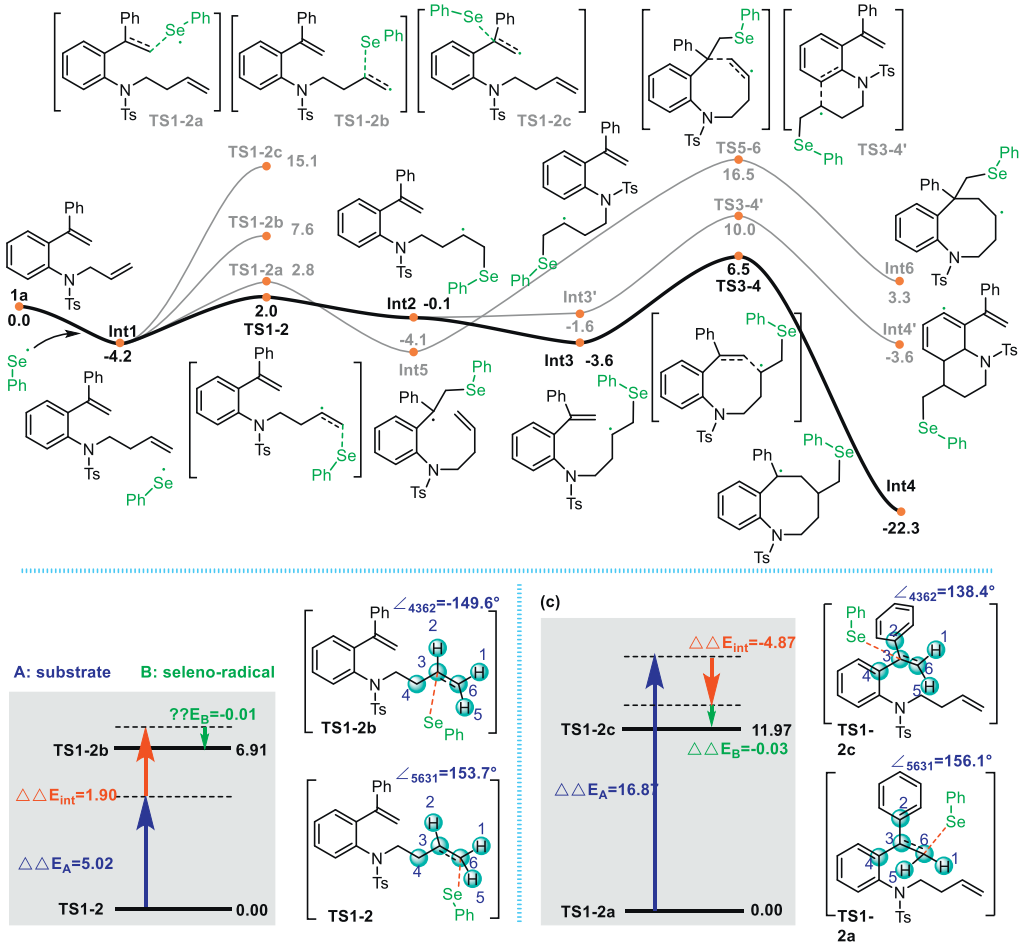

Fig. 3. The relative free energy profiles for the mechanism.

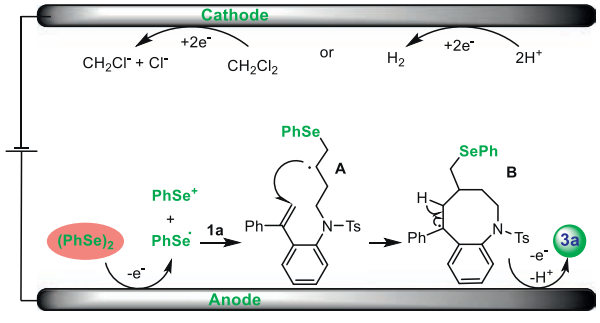

Scheme 6. Proposed mechanism.

which was similar to that of **2a** (1.98 V), consistent with Lei and co-workers' characterization of **2a** [66].

On the basis of these experimental results, we proposed a plausible reaction mechanism for the photo-induced 8-*endo* seleno-cyclization process (Scheme 6). First, anodic oxidation of $(PhSe)_2$ **2a** generates seleno-radical and seleno-cation intermediates. Steric effects most likely render the seleno-radical more inclined to react with the double bond of the butenyl group to form the favored radical intermediate **A**, which then undergoes an intramolecular 8-*endo* cyclization to deliver the radical intermediate **B**. Importantly, the competitive intramolecular 6-*endo* cyclization to a thermodynamically favorable quinoline scaffold (Scheme 1b, challenge ii) was not observed during the transformation. Subsequently, radical intermediate **B** rapidly undergoes one-electron oxidation at the anode and deprotonation to yield the desired 8-membered benzo[*b*]azocine **3a**. Meanwhile, the electrochemical reduction of the DCM solvent or proton occurs at the cathode to balance the overall charge state of the system.

Detailed density functional theory (DFT) calculations were performed using the Gaussian 16 package to gain additional mechanistic insights and to determine the origin of the observed chemoselectivity (Fig. 3, additional details in Supporting information). The DFT calculations first probed the reaction between the *in situ* generated seleno-radical and substrate **1a**. As shown in Fig. 3a, four potential transition states for the radical addition process could be located depending on the reaction site (*i.e.*, the double bonds in the butenyl group and diphenylethylene). Radical addition at the terminal carbons of the butenyl double bond (*via* **TS1–2**) and the diphenylethylene (*via* **TS1–2a**) faced lower reaction barriers compared with **TS1–2b** and **TS1–2c**. Energy decomposition analysis (Fig. 3b) for **TS1–2** and **TS1–2b** indicated that the high free energy barrier associated with **TS1–2b** could be ascribed to the large geometric distortion from the planer sp^2 carbon center to the tetrahedral *pseudo*-sp^3 carbon center (dihedral angels in **TS1–2b** and **TS1–2** measured as 149.6° and 153.7°, respectively). Similar results were obtained from the energy decomposition analysis of **TS1–2a** and **TS1–2c** (Fig. 3c), where the planer carbon center was distorted to 138.4° in **TS1–2c**. We also found that **Int2** could isomerize to **Int3** or **Int3'**; these two are primed for the subsequent intramolecular cyclization process. These DFT calculations indicated that the free energy barrier required for 8-*endo* cyclization *via* **TS3–4** was 10.7 kcal/mol, which is 3.5 kcal/mol more

favorable than that for the 6-*endo* cyclization *via* **TS3–4′**. In addition, the 8-*endo* cyclization intermediate **Int4** is thermodynamically more stable than **Int4'** by 18.7 kcal/mol. The DFT calculations also revealed that the cyclization of intermediate **Int5** to **Int6** is kinetically and thermodynamically unfavorable. Overall, the computational results support the 8-*endo* cyclization pathway, through which **Int4** can be further oxidized and deprotonated to yield the desired 8-membered benzo[*b*]azocine **3a**.

In conclusion, we developed a novel method for the electrochemically-driven chemoselective seleno-cyclization of dienes to prepare medium-sized benzo[*b*]azocines. After compensating for the inherently unfavorable enthalpic and entropic factors and variable chemoselectivity, we obtained 31 structurally diverse seleno-benzo[*b*]azepines in moderate to high yields at room temperature. The facile deselenation of the seleno-cyclization product to afford new functionalized dienes is an additional valuable feature of this reaction. The inhibition experiments, divided-cell experiments, and CV results were used to propose a plausible radical-based mechanism. DFT calculations further rationalized the rate-determining step and chemoselectivity observed in this transformation.

Declaration of competing interest

The authors declare that they have no known competing financial interests or personal relationships that could have appeared to influence the work reported in this paper.

Acknowledgments

This work was supported by the National Natural Science Foundation of China (No. 21801007) and Qingchuang Technology Support Program of University in Shandong Province (No. 2021KJ066). S.-F. Ni acknowledges funding from the STU Scientific Research Foundation for Talents (No. NTF20022).

Supplementary materials

Supplementary material associated with this article can be found, in the online version, at doi:10.1016/j.cclet.2023.109058.

References

[1] J.D. Brown, Comprehensive Heterocyclic Chemistry, Ch. 3, Pergamon Press, Oxford, 1984.
[2] P.A. Evans, B. Holmes, Tetrahedron 47 (1991) 9131–9166.
[3] T. Fukuyama, L. Xu, S. Goto, J. Am. Chem. Soc. 114 (1992) 383–385.
[4] M.L. Bennasar, E. Zulaica, D. Solé, S. Alonso, Chem. Commun. 23 (2009) 3372–3374.
[5] T. Toma, Y. Kita, T. Fukuyama, J. Am. Chem. Soc. 132 (2010) 10233–10235.
[6] L. Min, Y.J. Hu, J.H. Fan, et al., Chem. Soc. Rev. 49 (2020) 7015–7043.
[7] X.F. Kong, X.Y. Guo, Z.Y. Gu, et al., Org. Chem. Front. 7 (2020) 2055–2062.
[8] J.H. Fan, Y.J. Hu, L.X. Li, et al., Nat. Prod. Rep. 38 (2021) 1821–1851.
[9] G. Illuminati, L. Mandolini, Acc. Chem. Res. 14 (1981) 95–102.
[10] K. Sun, D.Y. Zhao, Q.X. Li, et al., Sci. China Chem. 66 (2023) 2309–2316.
[11] H. Ohno, H. Hamaguchi, M. Ohata, et al., Angew. Chem. Int. Ed. 42 (2003) 1749–1753.
[12] I. Shiina, Chem. Rev. 107 (2007) 239–273.
[13] L.G. Voskressensky, L.N. Kulikova, T.N. Borisova, et al., Adv. Heterocycl. Chem. 96 (2008) 81–122.
[14] A.V. Listratova, L.G. Voskressensky, Synthesis 49 (2017) 3801–3834.
[15] M.H. Shaw, R.A. Croft, W.G. Whittingham, J.F. Bower, J. Am. Chem. Soc. 137 (2015) 8054–8057.
[16] G. Fumagalli, S. Stanton, J.F. Bower, Chem. Rev. 117 (2017) 9404–9432.
[17] O. Boyd, G.W. Wang, O.O. Sokolova, et al., Angew. Chem. Int. Ed. 58 (2019) 18844–18848.
[18] O.O. Sokolova, J.F. Bower, Chem. Rev. 121 (2021) 80–109.
[19] R.T. Yu, R.K. Friedman, T. Rovis, J. Am. Chem. Soc. 131 (2009) 13250–13251.
[20] F. Miege, C. Meyer, J. Cossy, Angew. Chem. Int. Ed. 50 (2011) 5932–5937.
[21] S. Wu, R. Zeng, C. Fu, et al., Chem. Sci. 6 (2015) 2275–2285.
[22] P. Kumar, K. Zhang, J. Louie, Angew. Chem. Int. Ed. 34 (2012) 8602–8606.
[23] A. Thakur, M.E. Facer, J. Louie, Angew. Chem. Int. Ed. 52 (2013) 12161–12165.
[24] T.G. Minehan, Acc. Chem. Res. 49 (2016) 1168–1181.
[25] L. Pang, S.J. Fang, P.S. Zou, et al., Org. Chem. Front. 10 (2023) 1780–1787.
[26] S.J. Miller, S.H. Kim, Z.R. Chen, R.H. Grubbs, J. Am. Chem. Soc. 117 (1995) 2108–2109.
[27] M.S. Visser, N.M. Heron, M.T. Didiuk, et al., J. Am. Chem. Soc. 118 (1996) 4291–4298.
[28] L.A. Paquette, S.M. Leit, J. Am. Chem. Soc. 121 (1999) 8126–8127.
[29] G. Mugesh, W.W. du Mont, H. Sies, Chem. Rev. 101 (2001) 2125–2180.
[30] C.W. Nogueira, G. Zeni, J.B.T. Rocha, Chem. Rev. 104 (2004) 6255–6286.
[31] G. Perin, E.J. Lenardao, R.G. Jacob, R.B. Panatieri, Chem. Rev. 109 (2009) 1277–1301.
[32] A.J. Mukjerjee, S.S. Zade, H.B. Singh, R.B. Sunoj, Chem. Rev. 110 (2010) 4357–4416.
[33] K.P. Bhabak, G. Mugesh, Acc. Chem. Res. 43 (2010) 1408–1419.
[34] M. Ninomiya, D.R. Garud, M. Koketsu, Chem. Rev. 255 (2011) 2968–2990.
[35] E. Jablonska, M. Vinceti, J. Environ. Sci. Health. C: Environ. Carcinog. Ecotoxicol. Rev. 33 (2015) 328–368.
[36] X. Wang, Z.C. Wang, Z.J. Li, et al., Chin. Chem. Lett. 34 (2023) 108045–108058.
[37] K. Sun, X. Wang, C. Li, et al., Org. Chem. Front. 7 (2020) 3100–3119.
[38] H. Sahoo, A. Mandal, S. Dana, M. Baidya, Adv. Synth. Catal. 360 (2018) 1099–1103.
[39] Y.X. Xin, S. Pan, Y. Huang, et al., J. Org. Chem. 83 (2018) 6101–6109.
[40] K. Sun, S.N. Wang, R.R. Feng, et al., Org. Lett. 21 (2019) 2052–2055.
[41] Z.P. Ye, P.J. Xia, F. Liu, et al., J. Org. Chem. 85 (2020) 5670–5682.
[42] S. Mallick, M. Baidya, K. Mahanty, et al., Adv. Synth. Catal. 362 (2020) 1046–1052.
[43] X.L. Ma, Q. Wang, X.Y. Feng, et al., Green. Chem. 21 (2019) 3547–3551.
[44] J.D. Fang, X.B. Yan, L. Zhou, et al., Adv. Synth. Catal. 361 (2019) 1985–1990.
[45] J.W. Hua, Z. Fang, J. Xu, et al., Green. Chem. 21 (2019) 4706–4711.
[46] Z.P. Guan, Y.K. Wang, H.M. Wang, et al., Green. Chem. 21 (2019) 4976–4980.
[47] A. Kharma, C. Jacob, Í.A.O. Bozzi, et al., Eur. J. Org. Chem. 2020 (2020) 4474–4486.
[48] J.W. Hua, Z. Fang, M.X. Bian, et al., ChemSusChem 13 (2020) 2053–2059.
[49] L. Sun, L.W. Wang, H. Alhumade, et al., Org. Lett. 23 (2021) 7724–7729.
[50] H. Li, F.L. Lu, J. Xu, et al., Org. Chem. Front. 9 (2022) 2786–2791.
[51] K.A. Margrey, D.A. Nicewicz, Acc. Chem. Res. 49 (2016) 1997–2006.
[52] C. Qian, Q.S. Zheng, J. Chen, et al., Green. Chem. 25 (2023) 1368–1379.
[53] J.B. Sperry, D.L. Wright, Chem. Soc. Rev. 35 (2006) 605–621.
[54] J.I. Yoshida, K. Kataoka, R. Horcajada, A. Nagaki, Chem. Rev. 108 (2008) 2265–2299.
[55] B.A. Frontana-Uribe, R.D. Little, J.G. Ibanez, et al., Green. Chem. 12 (2010) 2099–2119.
[56] M. Yan, Y. Kawamata, P.S. Baran, Chem. Rev. 117 (2017) 13230–13319.
[57] K. Sun, Y. Li, T. Xiong, et al., J. Am. Chem. Soc. 133 (2011) 1694–1697.
[58] K. Sun, X. Wang, L. Liu, et al., ACS Catal. 5 (2015) 7194–7198.
[59] K. Sun, Y. Zhang, M. Tian, et al., Chem. Commun. 58 (2022) 9658–9661.
[60] M. Yu, Z. Zhou, Y. Chen, et al., Org. Lett. 24 (2022) 4886–4891.
[61] Z. Zhang, S. Wang, P. Tan, et al., Org. Lett. 24 (2022) 2288–2293.
[62] Z.L. Li, G.C. Fang, Q.S. Gu, X.Y. Liu, Chem. Soc. Rev. 49 (2020) 32–48.
[63] T.T. Wang, X.B. Jing, C. Chen, L. Yu, J. Org. Chem. 82 (2017) 9342–9349.
[64] P.Z. Li, Z.Y. Qi, L. Yu, H.W. Zhou, Catal. Sci. Technol. 12 (2022) 2241–2247.
[65] X.Y. Chen, J.F. Mao, C. Liu, et al., Chin. Chem. Lett. 31 (2020) 3205–3208.
[66] L. Sun, Y. Yuan, M. Yao, et al., Org. Lett. 21 (2019) 1297–1300.